

## Scalings and structures in turbulent Couette-Taylor flow

Zhen-Su She,<sup>1,2</sup> Kui Ren,<sup>1</sup> Gregory S. Lewis,<sup>3,\*</sup> and Harry L. Swinney<sup>3</sup>

<sup>1</sup>*State Key Laboratory for Turbulence Research, Department of Mechanical and Engineering Science, Peking University, Beijing 100871, People's Republic of China*

<sup>2</sup>*Department of Mathematics, UCLA, Los Angeles, California 90095*

<sup>3</sup>*Physics Department and Center for Nonlinear Dynamics, University of Texas at Austin, Austin, Texas 78712*

(Received 3 October 2000; published 18 June 2001)

The scaling of velocity structure functions in Couette-Taylor flow [Lewis and Swinney, Phys. Rev. E **59**, 5457 (1999)] is revisited to obtain more accurate values of the scaling exponents for the Reynolds number range investigated, 12 000 to 540 000 (Taylor Reynolds numbers,  $34 < R_\lambda < 220$ ). Systematic convergence of the statistics with increasing sample size is examined, and the uncertainty of the scaling exponents is assessed. At all Reynolds numbers the data support the hierarchical symmetry proposed by She and Leveque [Phys. Rev. Lett. **72**, 336 (1994)]. The She-Leveque constant  $\beta$  has a value of 0.83, indicating greater intermittency in Couette-Taylor turbulence than in free jets, where  $\beta=0.87$ . The constant  $\gamma$ , which is a measure of the degree of singularity of the most intermittent structure, decreases from 0.14 for  $R < 10^5$  to 0.10 for  $R > 10^5$ ; this transition corresponds to a visually observed break up of the Taylor vortex roll structure with increasing  $R$ .

DOI: 10.1103/PhysRevE.64.016308

PACS number(s): 47.27.Gs, 47.27.Jv, 05.45.Tp

### I. INTRODUCTION

At high Reynolds numbers, turbulent flows develop fluctuations over a range of scales in which the decay of statistical correlations is governed by power laws [1,2]. The power law exponents characterize a system, and their interpretation can lead to an understanding of the underlying physics, especially when intermittency is prominent.

Scaling laws for turbulent flows have been determined for several different geometries in recent years (see Ref. [3] and references therein). We consider here the turbulence that arises in flow between concentric cylinders with the inner cylinder rotating and the outer cylinder at rest (a Couette-Taylor system). We analyze velocity measurements obtained for Reynolds numbers ranging up to 540 000 (based on the gap between the cylinders) for a system with radius ratio 0.724 [4]. In the core of the turbulent flow, the small-scale structures generated through the turbulent cascade become mixed with the structures that develop near the wall and are swept into the bulk. Turbulence in such a closed system has a more complicated structure than turbulent flow in a free jet or wake. We will show that this difference is indicated by differences in the structure function exponents and in the parameter  $\beta$  in the She-Leveque hierarchical structure model [5].

One of the consequences of the mixed origin of small-scale structures in the bulk of the fluid may be the absence of an inertial range, even at moderately high Reynolds numbers. In our Couette-Taylor experiments [4], the Taylor Reynolds number based on the Taylor microscale is fairly large ( $R_\lambda \approx 220$ ), yet the velocity data do not exhibit any range with scaling (i.e., no inertial range), perhaps because flow structures originating from the wall are anisotropic and carry information from several scales when they are swept across

measurement probe. However, even with mixing of anisotropic structures, the method of extended self-similarity (ESS) [6] yields a wide scaling range [4]. This implies that once turbulent fluctuations are substantially developed, there exists a similarity property intrinsic to multiscale fluctuation fields.

In this study we obtain scaling exponents for the velocity structure functions from truncated velocity increment probability distribution functions (PDFs) rather than directly from velocity increments, and we examine the convergence of the exponent values as a function of the size of the data sets. These analyses lead to more accurate estimates for the exponents than obtained previously [4]. We apply the  $\beta$  test and the  $\gamma$  test of the hierarchical structure model [5,7,8] and find that the data obey the hierarchical symmetry assumed in the model. We will discuss the interpretation of the values determined for the model parameters  $\beta$  and  $\gamma$ .

In Sec. II we describe briefly the experiment and then argue that the structure function exponents can be obtained more accurately from truncated PDFs than from a direct Riemann sum. We also examine the convergence of estimates for the exponents as a function of the number of data points. In Sec. III we present results from the She-Leveque model: the  $\beta$  test and  $\gamma$  test. Section IV discusses the conclusions and suggests future directions.

### II. MEASUREMENTS AND CONVERGENCE STUDIES

Velocity measurements were made with a thermal velocity probe located midway between the two cylinders [4]. The root-mean-square velocity fluctuations were typically only 6% of the mean velocity so the Taylor frozen turbulence hypothesis should be accurate. Hence the temporal fluctuations recorded by the thermal velocimeter should reflect the streamwise spatial fluctuations, and consequently we will not distinguish between space and time in our analysis.

The main statistical quantities we consider are moments of the velocity differences, the velocity structure functions:

\*Present address: Calimetrics, Inc., Suite 105, 815 Atlantic Ave., Alameda, CA 94501.

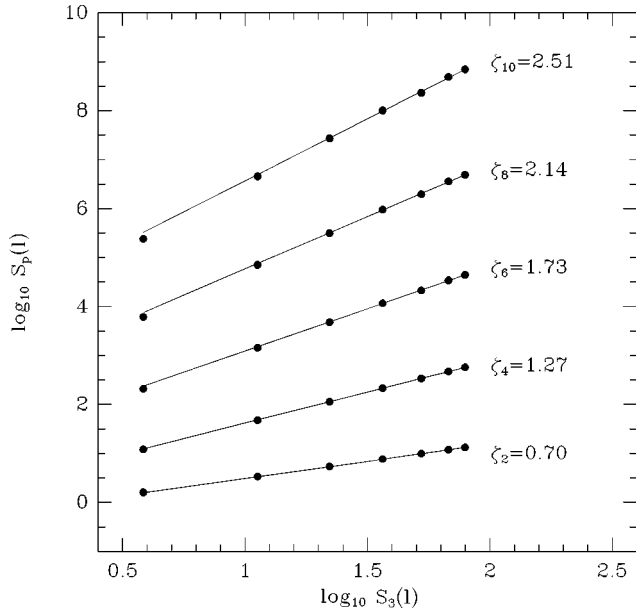


FIG. 1. ESS: over a range of scale of more than one decade ( $2^3 \delta \leq \ell \leq 2^8 \delta$ ) where  $\delta$  is the distance between the sample points, the log of the  $p$ th-order structure function varies linearly with the log of the third order structure function. These curves were made with  $2 \times 10^6$  data points, only one-tenth the length of our data set.  $R = 540\,000$ .

$S_p(\ell) = \langle |\delta v_\ell|^p \rangle$ , where  $\delta v_\ell = v(t + \ell) - v(t)$  is a velocity increment across a distance  $\ell$ , and both  $v$  and  $\ell$  are taken along the direction of the mean flow (the azimuthal direction). In a scaling analysis, the range of  $\ell$  examined is chosen such that the variation of  $S_p(\ell)$  follows a power law,  $S_p(\ell) \propto \ell^{\zeta_p}$ . However, in the flow examined here, there is no range of  $\ell$  for which a power law behavior of  $S_p(\ell)$  is observed, even at the highest Reynolds number studied [4], but there is a range in which the dependence  $S_p(\ell)$  on  $S_3(\ell)$  is described by a power law. This relative scaling is called ESS property of the velocity structure function in turbulence [6]. A typical ESS plot is shown in Fig. 1. Remarkably, we find that even with only one-tenth of our total data, there exists a range for which the ESS plots exhibit scaling behavior. At  $R = 540\,000$ , the range over which the ESS holds is one and a half decades in  $\ell$ . If those scales were in the asymptotic inertial range, the third order moments would vary also over a decade and a half, but for our data the third order moments exhibit no scaling range when plotted directly as a function of  $l$ . However, in ESS the length scale  $\ell$  is implicit. Over this implicit range the nonlinear transfer (or cascade) is presumably important, but there is no theory of the ESS property. Such a theory should predict, among other things, where the ESS property fails.

When turbulence is maintained in a statistically stationary state, an ensemble average is customarily replaced with a time average by the ergodic hypothesis. Thus  $S_p(\ell)$  is calculated by integration in time,

$$S_p(\ell) = \frac{1}{T} \int_0^T [\delta v_\ell(t)]^p dt. \quad (1)$$

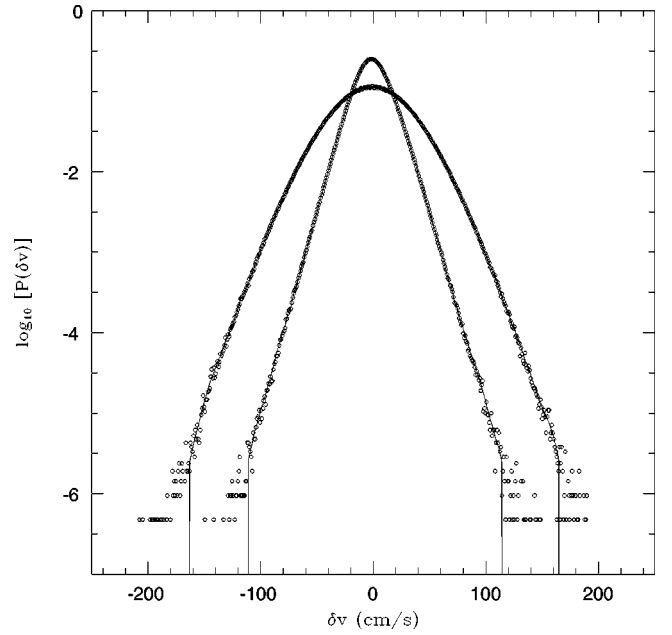


FIG. 2. Probability distribution functions of the velocity increments at two length scales ( $2^3 \delta$  and  $2^8 \delta$ , where  $\delta$  is the distance between data points, 0.17 mm). Points and lines are the PDFs without and with the noise reduction procedure applied, respectively.  $R = 540\,000$ ,  $2 \times 10^7$  points.

This calculation is susceptible to errors for high order moments because for large  $p$  (say  $p \geq 10$ ) a spurious large fluctuation can change the results considerably. How can a spurious large measurement be distinguished from a genuine large fluctuation? Large fluctuations are still smooth variations in time; hence the PDF should vary smoothly, even in the tails. We remove improbable events from the PDFs by first constructing a histogram of the velocity increment  $\delta v_\ell$  and normalizing it to make a PDF,  $P(\delta v_\ell)$ . Typical PDFs of  $\delta v_\ell$  at two scales  $\ell$  are shown in Fig. 2. The discrete dots in the tails correspond to events that occur only a few times (in a total of more than ten million data points), a consequence of the finite sample size. An event that appears only once (or a few times) in the entire time record is not statistically significant. Our noise reduction procedure consists in eliminating the few lowest discrete probability density events: the probability density is set to zero below a threshold of  $5 \times p_{min}$ , where  $p_{min}$  is the lowest probability density due to the finite sample size ( $p_{min} = c/N$ ), where  $N$  is the number of data points and  $c$  is a constant depending on the discretization of  $\delta v_\ell$  when constructing the histograms. In Fig. 3 we show PDFs obtained with application of the noise reduction procedure for three different sample sizes.

The structure functions are now evaluated by a direct integration with the PDFs,

$$S_p(\ell) = \int_{-\infty}^{\infty} |\delta v_\ell|^p P(\delta v_\ell) d(\delta v_\ell). \quad (2)$$

Figure 4 compares extended self-similarity scaling of structure functions for three values of  $p$ , plotted with and without applying the noise reduction procedure. Before reducing the

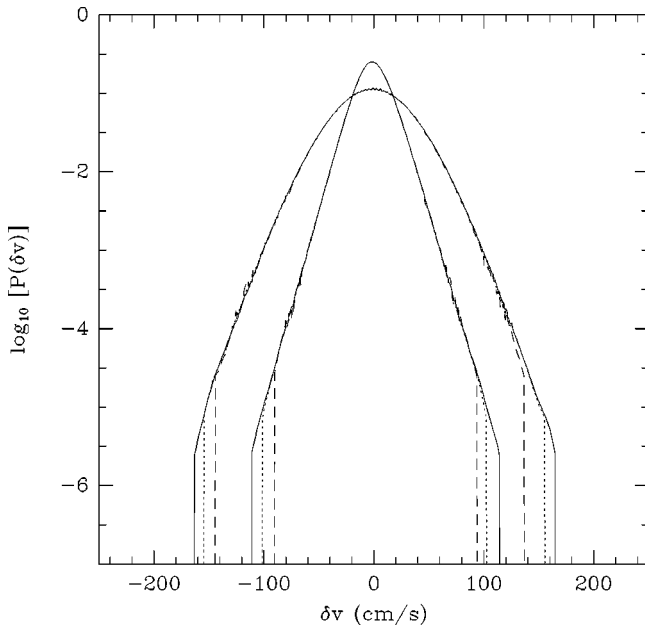


FIG. 3. PDFs of the velocity increment with the noise reduction procedure applied for three sample sizes:  $2 \times 10^6$  points, dashed line;  $6 \times 10^6$  points, dotted line; and  $2 \times 10^7$  points, solid line. As the sample size increases, the tail of the PDF extends further.

noise, the moments exhibit large fluctuations due to the appearance of improbable extreme events. After reducing the noise, the fluctuations are much smaller, suggesting that the statistical ensemble for the smoothed fluid structures exhibits

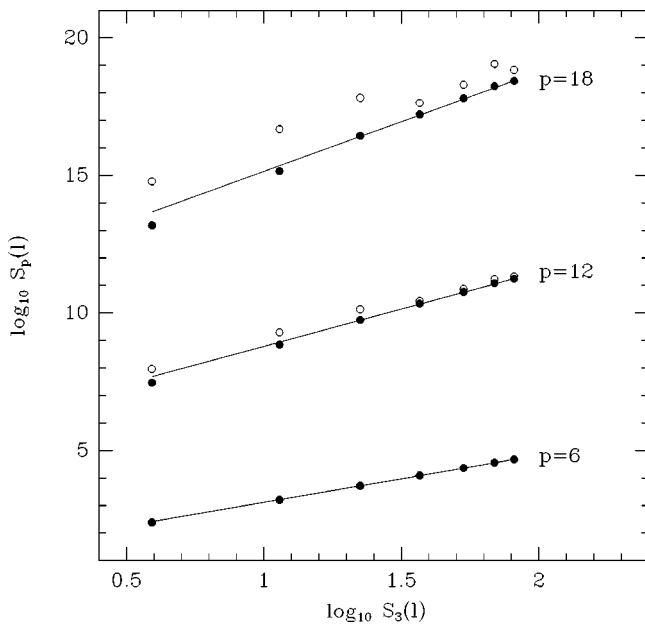


FIG. 4. Comparison of the relative scaling ESS calculated using the PDFs with the noise reduction procedure (filled symbols) to those without the noise reduction procedure (open symbols). After noise reduction, the moments fluctuate much less with  $S_3(\ell)$  (or with  $\ell$ ) and the dependence is described by a power law. The lines are the least square fits from which the scaling exponents were extracted.  $R = 540\,000$ ,  $2 \times 10^7$  points.

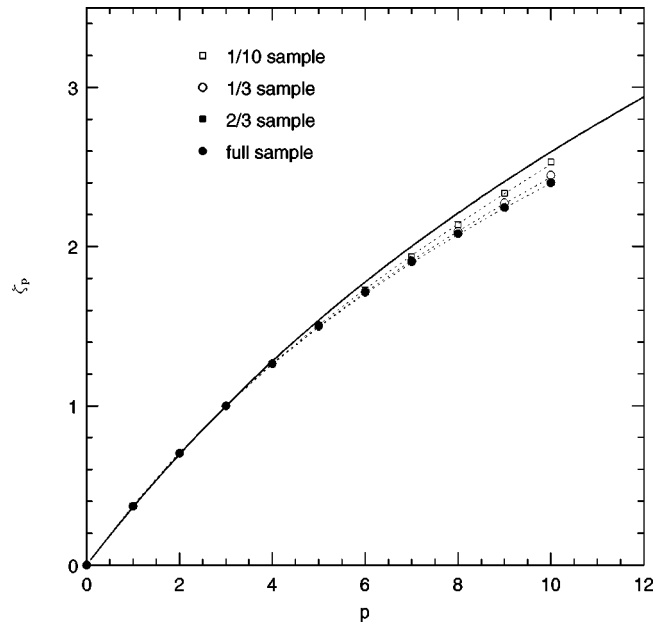


FIG. 5. Structure function exponents  $\zeta_p$  for one-tenth, one-third, and all of the data ( $2 \times 10^7$  points) at  $R = 540\,000$ . The dashed lines show the prediction of the She-Leveque model with our measured values of  $\beta$  and  $\gamma$ , and the solid line shows the prediction of the She-Leveque model with  $\beta = (2/3)^{1/3}$  and  $\gamma = 1/9$ , as for fully turbulent flow of a jet.

extended self-similarity even for very high order moments, up to  $p = 18$ . All structure function calculations that we will present were conducted using the noise reduction procedure.

We next consider the convergence of the structure function exponents  $\zeta_p$  with the size of the data set; Anselmetti *et al.* [9] pointed out the importance of testing for this convergence. The convergence of the scaling exponent values may be different from the convergence of the moments—scaling exponents could converge faster because they characterize the rate of change of the logarithm of moments. There is no theory to assess the error bars in exponents. The study of sample size dependence is a tangible way to assess the uncertainty in the exponents. A typical result is shown in Fig. 5 in which the ESS scaling exponents are calculated with one-tenth, one-third, and the full sample size at  $R = 540\,000$ : the  $\zeta_p$  values decrease as the sample size increases. A smaller value of  $\zeta_p$  marks a larger departure from a Kolmogorov 1941 value, and hence larger intermittency effects. This is understandable since as the sample size increases, larger (presumably more intermittent) fluctuation amplitudes are included. We find that for  $p \leq 10$ ,  $\zeta_p$  has converged within one or two percent (symbols in Fig. 5 overlap), but for  $p > 10$ , longer time series are needed to ensure convergence.

If the velocity signal is not recorded long enough, the values of the scaling exponents  $\zeta_p$  will be systematically larger, as Fig. 5 shows. Antonia and Shafi [10] studied the scaling in a rough wall turbulent boundary layer and obtained slightly larger values of  $\zeta_p$  than the original She-Leveque values. This may partly be due to a too small data set ( $10^6$  points, about 1/20 of our data set). In view of the result

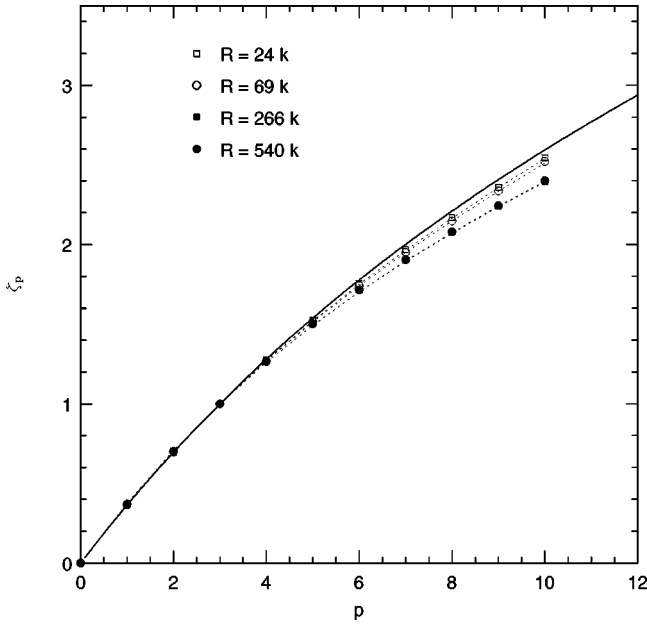


FIG. 6. Structure function exponents  $\zeta_p$  measured at four values of  $R$ :  $2.4 \times 10^4$  (open squares),  $6.9 \times 10^4$  (open circles),  $2.66 \times 10^5$  (solid squares), and  $5.4 \times 10^5$  (solid circles); the  $\zeta_p$  at the latter two  $R$  are indistinguishable on the scale of the graph. The dashed lines are the She-Leveque formula with our measured values of  $\beta$  and  $\gamma$ . The solid line shows the prediction of the She-Leveque model with  $\beta = (2/3)^{1/3}$  and  $\gamma = 1/9$ , which accurately describe the scaling exponents for turbulent open jets and wakes.

presented above, it may be stated that their exponents have not fully converged. On the other hand, a difference between the Couette-Taylor flow and the rough wall boundary flow is possible, which we will discuss more in the Sec. IV.

Similar analyses were carried out for all sets of data for  $1.2 \times 10^4 \leq R \leq 5.4 \times 10^5$ . At each Reynolds number PDFs were constructed for velocity differences at scales from  $2^1 \delta$  to  $2^{10} \delta$ , where  $\delta$  is the distance between the data points. Then, the noise reduction procedure was applied and moments were computed. ESS plots helped in identifying the range of scaling behavior, which was typically  $2^3 \delta \leq l \leq 2^8 \delta$ , where  $\delta = 0.17$  mm, the distance between sample points. Scaling exponents  $\zeta_p$  were obtained by a least square fit in the chosen range. Each data set was treated starting with a fraction of the sample size to the full sample size in order to assess the convergence; the results presented in the next section are considered to be converged with respect to sample size dependence.

### III. RESULTS

Figure 6 presents the structure function exponents,  $p \leq 10$ , at four Reynolds numbers. The  $\zeta_p$  values for  $R < 10^5$  are larger than for  $R > 10^5$ . Within the statistical uncertainty (less than the size of a symbol on the graph), the exponents at the two larger values of  $R$  are the same, which suggests that the values have converged as a function of  $R$ , although this cannot be guaranteed without obtaining data for yet larger  $R$ . The  $\zeta_p$  at the larger  $R$  in Fig. 6 are smaller than

predicted by the original She-Leveque model [5], which has been found to describe the scaling exponents in free jets and wakes [11].

#### A. The $\beta$ test

At all Reynolds numbers the scaling exponents in Fig. 6 are remarkably well described by a generalized She-Leveque formula with parameters  $\beta$  and  $\gamma$  determined, not by a fitting procedure, but by well-defined procedures called the “ $\beta$  test” and the “ $\gamma$  test.” These techniques have recently been introduced and used by She *et al.* [8] to analyze turbulence data obtained in experiments [12] and numerical simulations [13–15]. We now describe the  $\beta$  test and  $\gamma$  test in turn.

The hierarchical structure model of She and Leveque [5,7] involves a hierarchy of functions  $F_p(\ell) = S_{p+1}(\ell)/S_p(\ell)$ , each describing more closely the intensity of fluctuations [5].  $F_p(\ell)$  is associated with higher intensity fluctuations with increasing  $p$ . She and Leveque [5] postulated an invariant relation between  $F_p$  and  $F_{p+1}$ , which is referred to as a hierarchical symmetry relation (a symmetry with respect to a translation in  $p$ ),

$$F_{p+1}(\ell) = A_p F_p(\ell)^\beta F_\infty(\ell)^{1-\beta}, \quad (3)$$

where  $0 \leq \beta \leq 1$  is a constant and  $A_p$  is independent of  $\ell$  and may also be nearly independent of  $p$ . The most intermittent structures are characterized by

$$F_\infty(\ell) = \lim_{p \rightarrow \infty} \langle |\delta v_\ell|^{p+1} \rangle / \langle |\delta v_\ell|^p \rangle \quad (4)$$

because it is associated with the most intense fluctuation events. The term  $F_\infty(\ell)^{1-\beta}$  can be eliminated by considering the ratio

$$\frac{F_{p+1}(\ell)}{F_2(\ell)} = \frac{A_p}{A_1} \left( \frac{F_p(\ell)}{F_1(\ell)} \right)^\beta. \quad (5)$$

If a log-log plot of  $F_{p+1}(\ell)/F_2(\ell)$  vs  $F_p(\ell)/F_1(\ell)$  is a straight line, we say that the data pass the  $\beta$  test because the assumed hierarchical symmetry is satisfied. Then the value of  $\beta$  is the slope of the line. In Fig. 7 we show the result of the  $\beta$  test for the Couette-Taylor data at four Reynolds numbers.

The parameter  $\beta$  measures the degree of intermittency of a turbulent flow. In the limit  $\beta \rightarrow 1$ , there is no intermittency. The Kolmogorov 1941 picture of turbulence belongs to this limit, and it is straightforward to show that  $\zeta_p \rightarrow p/3$  [see Eq. (7) below]. In contrast, in the limit  $\beta \rightarrow 0$ , only the most intermittent structures persist; this is the ordered limit. One example in this category is the black and white  $\beta$  model [16] where only one type of structure (white) is responsible for the energy dissipation. A particular successful case of the black-white model is a random distribution of Burgers shocks whose energy spectrum is  $k^{-2}$  and whose scaling exponents are  $\zeta_p = 1$  for  $p \geq 1$  [17].

Our measured value of  $\beta$  (0.83) indicates that the Couette-Taylor turbulence is a mixture of order and disorder; this suggests that high intensity structures are partially cor-

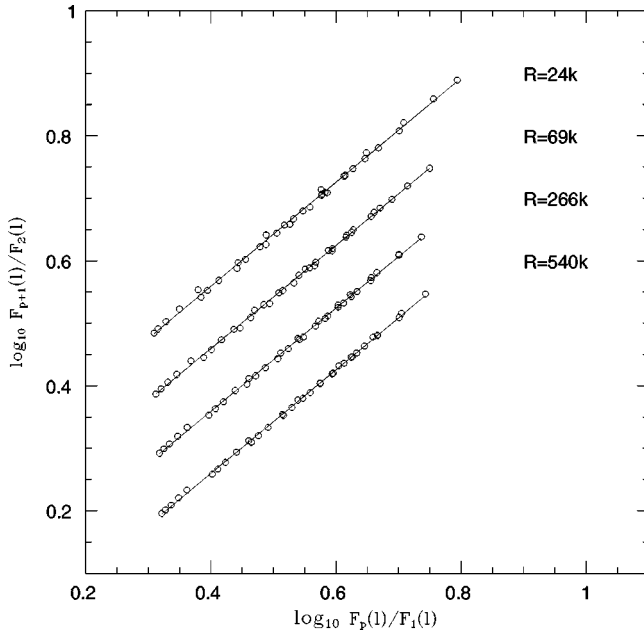


FIG. 7. The Couette-Taylor data at four  $R$  satisfy well the  $\beta$  test: each set of points is described by a straight line. Moreover, the value of  $\beta$  (slopes of the lines), is the same at each  $R$ , 0.83, somewhat smaller than in free jets ( $\beta \approx 0.87$ ). For clarity, points at different Reynolds numbers are separated by a suitable vertical displacement.

related with low intensity structures and they are partially similar. The absence of a dependence of  $\beta$  on Reynolds number suggests that the difference in similarity between them (we will call it the degree of intermittency) does not vary in the range of  $R$  studied.

### B. The $\gamma$ test

Once the statistics pass the  $\beta$  test, if one further assumes that

$$F_\infty \sim S_3^\gamma, \quad (6)$$

it can be shown that the general scaling formula [5] (with  $\zeta_3 = 1$ ) is given by

$$\zeta_p = \gamma p + C(1 - \beta^p), \quad (7)$$

where  $C = (1 - 3\gamma)/(1 - \beta^3)$ . Then simple algebraic manipulation gives

$$\zeta_p - \chi(p; \beta) = \gamma(p - 3\chi(p; \beta)), \quad (8)$$

where  $\chi(p; \beta) = (1 - \beta^p)/(1 - \beta^3)$ . If a plot of  $\zeta_p - \chi(p; \beta)$  vs  $p - 3\chi(p; \beta)$  yields a straight line, this confirms the assumption (6). The slope of the line in this “ $\gamma$  test” is the value of  $\gamma$ .

Figure 8 presents the results of the  $\gamma$  test for four Reynolds numbers. At each  $R$  the data yield a straight line; thus the data pass the  $\gamma$  test. Note that in order to conduct the  $\gamma$  test, the data must first pass the  $\beta$  test and yield a value of  $\beta$ . Then the measured  $\beta$  and  $\zeta_p$  are used in applying the  $\gamma$  test.

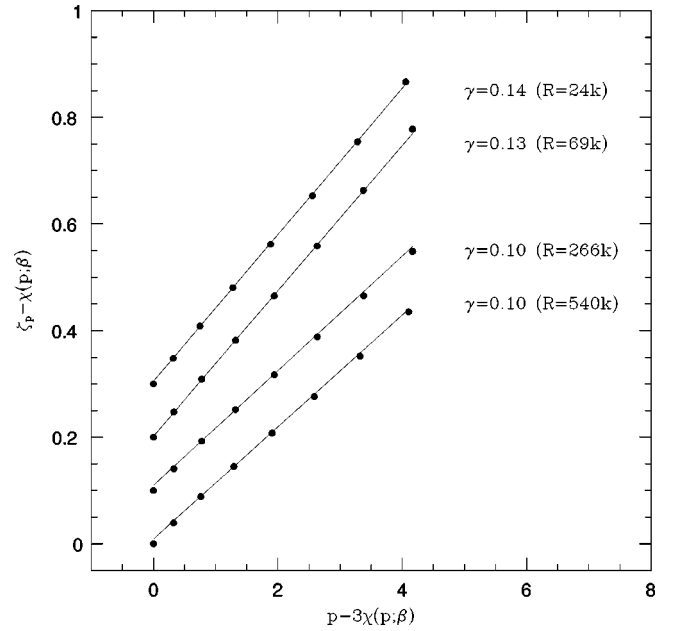


FIG. 8. The linearity of these curves demonstrates that the Couette-Taylor data pass the  $\gamma$  test. Note that  $\gamma \approx 0.14$  for  $R < 10^5$  and  $\gamma \approx 0.10$  for  $R > 10^5$ . For clarity, points at different Reynolds numbers are separated by a suitable vertical displacement.

$\gamma$  is a measure of the degree of singularity of the most intermittent structure  $F_\infty$ . If the most intermittent structures were shocks, then  $\gamma$  would be zero (the velocity difference across a shock discontinuity is proportional to  $\ell^0$ , or independent of  $\ell$ ). This is a strong singularity. An example of a weaker singularity is a velocity profile like Brownian motion for which  $\gamma = 1/2$ . The larger  $\gamma$  is, the weaker the singularity of the most intermittent structures. Kolmogorov’s dissipative structure has  $\gamma = 1/3$  (because for  $p$  large,  $\zeta_p^{K41} = p/3 = \gamma p$ ); therefore,  $K41$  dissipative structure is less singular than the shocks. In other words, Burgers turbulence is more intermittent than the Kolmogorov turbulence.

Although  $\gamma$  is theoretically a property of the very high-order moments,  $p \rightarrow \infty$  [see Eq. (4)], we find in analyses of simulations and experiments that a modest range of  $p$  ( $3 \leq p \leq 10$ ) can define the most intermittent structures. This is because the structures that contribute to  $F_p(\ell)$  for  $3 \leq p \leq 10$  comprise most of the intensive fluctuations that are statistically significant.  $\gamma$  is characteristic of those structures in the finite (but long) velocity record.

The change in the value of  $\gamma$  from 0.14 for  $R < 10^5$  to 0.10 for  $R > 10^5$  suggests that the most intermittent structures undergo a transition at  $R \approx 10^5$ . In Table I we list the measured values of  $\gamma$  for all Reynolds numbers. The robustness of the transition at  $R \approx 10^5$  and the convergence of the values of  $\beta$  and  $\gamma$  with data sets of increasing size are illustrated in Fig. 9. The values of  $\beta$  and  $\gamma$  from two-thirds of the data set and from the full data set coincide, indicating a convergent evaluation of  $\beta$  and  $\gamma$ . Even for smaller data sets where  $\beta$  and  $\gamma$  have not fully converged, the qualitative behavior of  $\beta$  and  $\gamma$  with increasing Reynolds number is the same, namely,  $\beta$  remains unchanged, but  $\gamma$  undergoes a transition at  $R \approx 10^5$ . This suggests that the  $\beta$  test and  $\gamma$  test can be applied

TABLE I. Measured She-Leveque parameters  $\beta$  and  $\gamma$  at different Reynolds numbers. The values of the Taylor microscale  $\lambda_T$  and the Taylor microscale Reynolds numbers  $R_\lambda$  are from formulas in [4]:  $R_\lambda = 0.324R^{0.495}$  and  $\lambda_T = 47.0R^{-0.473}$  cm. The Taylor microscale  $\lambda_T$  is much larger than the Kolmogorov dissipation scale  $\eta$ , which is 0.075 cm at  $R = 12\,000$  and 0.0057 cm at  $R = 540\,000$  (cf. Fig. 12 of [4]).

Reynolds number	$R_\lambda$	$\lambda_T$ (cm)	$\beta$	$\gamma$
12000	34	0.55	0.83	0.12
24000	48	0.40	0.83	0.14
34000	57	0.34	0.83	0.14
48000	67	0.29	0.83	0.14
69000	80	0.24	0.83	0.13
133000	110	0.18	0.83	0.10
266000	160	0.13	0.83	0.10
540000	220	0.09	0.83	0.10

even to small data sets to detect relative changes in the statistical structures of turbulent flows.

We speculate that the transition in  $\gamma$  around  $R \approx 10^5$  corresponds to a loss of coherence of the Taylor vortices. Visual observations indicate that when  $R$  is increased above about  $10^5$ , the Taylor vortices begin to break up and no longer have a well-defined structure [4]. The resultant structures are more turbulent and less ordered, hence more singular, and  $\gamma$  decreases.

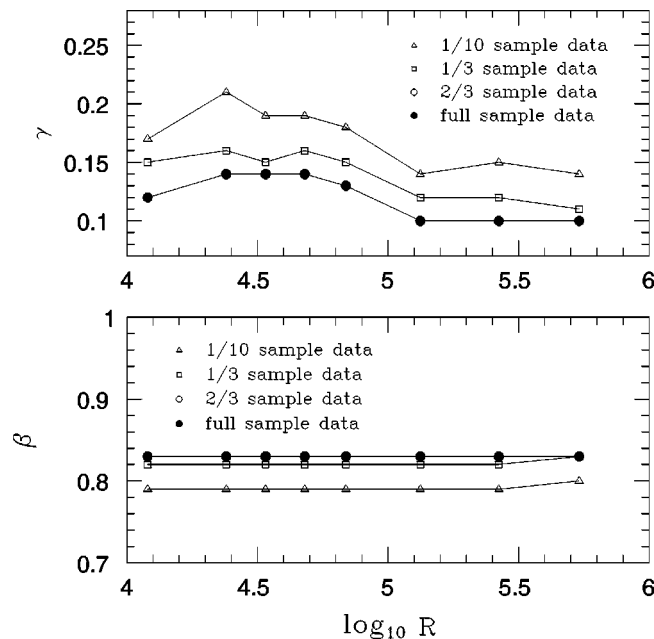


FIG. 9. The variation of  $\beta$  and  $\gamma$  as a function of the Reynolds number for four different data sizes. The results at two-thirds data set and the full data set completely coincide, suggesting the convergence. Note also a similar qualitative behavior for all data sizes.

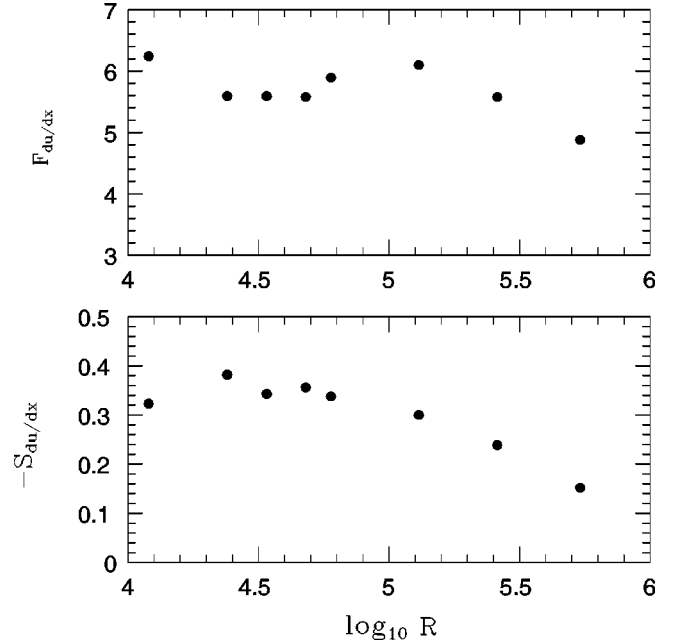


FIG. 10. Velocity derivative skewness ( $S_3$ ) and flatness ( $F$ ) as a function of the Reynolds number. Note the decreasing trend for  $R > 100\,000$ .

#### IV. DISCUSSION

We have analyzed velocity data for Couette-Taylor flow for a wide range of Reynolds number. The data are collected midway between the two cylinders and therefore reflect the property of the bulk turbulence. The scaling of the structure function for Couette-Taylor turbulence is found to be different from that for turbulent free jets or wakes (cf. Fig. 6). Further evidence that Couette-Taylor turbulence is different lies in the Reynolds number dependence of the velocity derivative flatness and skewness (Fig. 10), which both decrease with  $R$  for  $R > 100\,000$ ; this is opposite to the trend found in turbulent jets and wakes and in many other turbulent flows [18]. This difference merits further study. It may be due to the effects of rotation and the induced complex interaction between the flow structures originating from the Taylor vortices and from the boundary layer.

Structure functions were deduced not from Riemann sums but from PDFs that were reduced in noise by removing statistically insignificant points. Structure function exponents  $\zeta_p$  were determined by the method of extended self-similarity, and the  $\zeta_p$  values for  $p \leq 10$  were shown to have converged when increasing the length of the velocity time series. The  $\zeta_p$  values are smaller than the values previously reported for free jets or wakes, indicating that Couette-Taylor flow is more intermittent.

Couette-Taylor turbulence is well described by the hierarchical structure (HS) model, passing both the  $\beta$ -test and the  $\gamma$ -test. The HS model has an invariance (called hierarchical symmetry) that defines a transformation group [7]; this symmetry can be exactly simulated by a log-Poisson cascade process [19,20], so the model is also called the ‘‘log-Poisson’’ model. The HS model has previously been found to describe scaling exponents in several turbulent flows

[11,13,21,22]. The results here further suggest that the hierarchical symmetry is a general property of fully developed turbulent flows.

The  $\beta$  test yielded a value for the model parameter  $\beta$  that was found to be independent of Reynolds number. This suggests that in the Couette-Taylor flow, the weak and strong fluctuations have a different cascade property (i.e.,  $\beta \neq 1$ ), but that difference remains unchanged in the range of the Reynolds numbers studied. Our value of  $\beta$ , 0.83, is somewhat smaller than the one obtained in a free jet and in numerical simulations, where  $\beta \approx 0.87$ . We cannot say how significant this difference is; further study is warranted, e.g., by applying the  $\beta$  test and  $\gamma$  test on data sets of comparable size.

Further, we found that the parameter  $\gamma$  describing the most intermittent structures decreases from 0.14 to 0.11 near  $R = 10^5$ , which suggests that there is a transition at  $R \approx 10^5$  where the most intermittent structures become more singular. There is also a suggestion of this transition in the values of  $\zeta_p$  (Fig. 6). We believe that this transition corresponds to a visually observed breakup of the Taylor vortex roll structure with increasing  $R$  that initiates a cascade process yielding more singular small-scale structures. The detection of such a transition, if confirmed, is a significant step in the statistical

analysis of turbulent flows: we have a set of statistical measures ( $\beta$  and  $\gamma$ ) capable of capturing the structural transition in a fully developed turbulent regime.

Future experiments should collect longer velocity time series than ours ( $2 \times 10^7$  points). Longer files will yield events further in the tail of the distribution function, making it possible to obtain convergent values for  $\zeta_p$  for  $p > 10$ . In addition, velocity data should be obtained at different spatial locations, especially close to the walls where  $\gamma$  is expected to vary because the flow will depart increasingly from homogeneous isotropic turbulence. Finally, other flow geometries should be investigated to quantify the intermittent structures by applying the  $\beta$  test and the  $\gamma$  test.

#### ACKNOWLEDGMENTS

This work benefitted from discussions at the State Key Laboratory for Turbulence Research at Peking University, especially with Professor Shida Liu, Professor Qinding Wei, Professor Jiezhi Wu, and Dr. Weidong Su and Dr. Zhenping Zou. This work was partially supported by a grant from National Natural Science Foundation (NNSF) of China and from the Ministry of Education of China. G.S.L. and H.L.S. were supported by the U.S. Office of Naval Research.

- 
- [1] U. Frisch, *Turbulence: The Legacy of A. N. Kolmogorov* (Cambridge University Press, Cambridge, England, 1995).
- [2] K.R. Sreenivasan, *Annu. Rev. Fluid Mech.* **23**, 539 (1991).
- [3] A. Arneodo *et al.*, *Europhys. Lett.* **34**, 411 (1996).
- [4] G.S. Lewis and H.L. Swinney, *Phys. Rev. E* **59**, 5457 (1999).
- [5] Z.-S. She and E. Leveque, *Phys. Rev. Lett.* **72**, 336 (1994).
- [6] R. Benzi, S. Ciliberto, R. Tripicciono, C. Baudet, and S. Succi, *Phys. Rev. E* **48**, 29 (1993); R. Benzi, S. Ciliberto, C. Baudet, and G. Ruiz Chavarria, *Physica D* **80**, 385 (1995).
- [7] Z.-S. She, *Prog. Theor. Phys.* **130**, 87 (1998).
- [8] Z.-S. She and L. Liu (unpublished); Z.-S. She, L. Liu, and Z.-P. Zou (unpublished).
- [9] F. Anselmet, Y. Gagne, E.J. Hopfinger, and R.A. Antonia, *J. Fluid Mech.* **140**, 63 (1984).
- [10] R.A. Antonia and H.S. Shafi, *Exp. Fluids* **26**, 145 (1999).
- [11] R. Benzi, S. Ciliberto, C. Baudet, and G. Ruiz Chavarria, *Physica D* **80**, 385 (1995); R. Benzi, L. Biferale, S. Ciliberto, M.V. Struglia, and R. Tripicciono, *ibid.* **96**, 162 (1996).
- [12] F. Belin, P. Tabeling, and H. Willaime, *Physica D* **93**, 52 (1996).
- [13] N. Cao, S. Chen, and Z.-S. She, *Phys. Rev. Lett.* **76**, 3711 (1996).
- [14] E. Leveque and Z.-S. She, *Phys. Rev. Lett.* **75**, 2690 (1995).
- [15] E. Leveque and Z.-S. She, *Phys. Rev. E* **55**, 2789 (1997).
- [16] U. Frisch, M. Nelkin, and P.-L. Sulem, *J. Fluid Mech.* **87**, 719 (1978).
- [17] Ya.G. Sinai, *Commun. Math. Phys.* **148**, 601 (1992); Z.-S. She, E. Aurell, and U. Frisch, *ibid.* **148**, 623 (1992).
- [18] K.R. Sreenivasan and R.A. Antonia, *Annu. Rev. Fluid Mech.* **29**, 435 (1997).
- [19] B. Dubrulle, *Phys. Rev. Lett.* **73**, 959 (1994).
- [20] Z.-S. She and E.C. Waymire, *Phys. Rev. Lett.* **74**, 262 (1995).
- [21] G. Ruiz Chavarria, C. Baudet, and S. Ciliberto, *Phys. Rev. Lett.* **74**, 1986 (1995); G. Ruiz Chavarria, C. Baudet, R. Benzi, and S. Ciliberto, *J. Phys. II* **5**, 485 (1995).
- [22] D. Queros-Conde, *Phys. Rev. Lett.* **78**, 4426 (1997).